AIP Advances

Magnetic nanobeads present during enzymatic amplification and labeling for a simplified DNA detection protocol based on AC susceptometry

Rebecca S. Bejhed, Maria Strømme, Peter Svedlindh, Annika Ahlford, and Mattias Strömberg

Citation: AIP Advances **5**, 127139 (2015); doi: 10.1063/1.4939570
View online: http://dx.doi.org/10.1063/1.4939570
View Table of Contents: http://scitation.aip.org/content/aip/journal/adva/5/12?ver=pdfcov
Published by the AIP Publishing

Magnetic nanobeads present during enzymatic amplification and labeling for a simplified DNA detection protocol based on AC susceptometry

Rebecca S. Bejhed,[1] Maria Strømme,[1] Peter Svedlindh,[1] Annika Ahlford,[2] and Mattias Strömberg[1,a]

[1]*Department of Engineering Sciences, Uppsala University, Ångström Laboratory, Uppsala, Sweden*

[2]*Department of Biochemistry and Biophysics, Stockholm University, Science for Life Laboratory, Solna, Sweden*

(Received 2 October 2015; accepted 22 December 2015; published online 31 December 2015)

Magnetic biosensors are promising candidates for low-cost point-of-care biodiagnostic devices. For optimal efficiency it is crucial to minimize the time and complexity of the assay protocol including target recognition, amplification, labeling and read-out. In this work, possibilities for protocol simplifications for a DNA biodetection principle relying on hybridization of magnetic nanobeads to rolling circle amplification (RCA) products are investigated. The target DNA is recognized through a padlock ligation assay resulting in DNA circles serving as templates for the RCA process. It is found that beads can be present during amplification without noticeably interfering with the enzyme used for RCA (phi29 polymerase). As a result, the bead-coil hybridization can be performed immediately after amplification in a one-step manner at elevated temperature within a few minutes prior to read-out in an AC susceptometer setup, i.e. a combined protocol approach. Moreover, by recording the phase angle $\xi = \arctan(\chi''/\chi')$, where χ and χ'' are the in-phase and out-of-phase components of the AC susceptibility, respectively, at one single frequency the total assay time for the optimized combined protocol would be no more than 1.5 hours, often a relevant time frame for diagnosis of cancer and infectious disease. Also, applying the phase angle method normalization of AC susceptibility data is not needed. These findings are useful for the development of point-of-care biodiagnostic devices relying on bead-coil binding and magnetic AC susceptometry. [http://dx.doi.org/10.1063/1.4939570]

I. INTRODUCTION

In recent years, much research has focused on nanomaterials and their ability to elevate the performance of various biosensor techniques used in diagnostic applications.[1] One prominent nanomaterial emerging from these studies is magnetic nanoparticles.[2–4] Apart from requirements concerning sensitivity, selectivity and reliability, biosensors should ideally also be easy to handle and provide a fast response.[5,6] Furthermore, integration and automation of all reaction steps in sample preparation with sample analysis is essential for successful development of a fully automated diagnostic test. The possibility to implement such a test is much dependent on the simplicity of the assay. For instance, a homogeneous assay including as few steps and/or changes in variables as possible is desirable and integration of complex multistep protocols has been challenging to date.[7] Hence, magnetic micro- and nanoparticles have been proven useful for automation of sample preparation in bioanalytical devices by serving as solid phase supports to enable reagent exchange and washing in multi-step assays.[8,9]

[a]Electronic mail: mattias.stromberg@angstrom.uu.se

Magnetic biosensors, usually classified as either surface or volume based, are potential candidates for low-cost biodiagnostic devices operating in outpatient and point-of-care settings including applications such as infectious diagnostics,[10] food safety[11] and drinking water quality assessment.[12] Surface-based methods typically utilize thin film magnetic sensor elements functionalized with biomolecular probes and are therefore only sensitive to magnetic nanoparticles in the close vicinity to the sensor surface.[13] In contrast, volume-based sensors probe the entire sample volume and offer a convenient homogeneous readout format. One type of volume-based magnetic biosensing relies on measuring the decrease in Brownian relaxation frequency upon probe-target binding (e.g. an antigen-antibody reaction) occurring on the surface of magnetic nanobeads.[14,15]

In 2008 we demonstrated a refined and improved version of this approach for detection of DNA target sequences.[16] The assay protocol begins with highly specific target recognition through padlock probe ligation forming DNA circles. Thereafter, the circles serve as templates for isothermal rolling circle amplification (RCA, typically for 60 min at 37°C) generating macromolecular single stranded DNA coils (size about 1 μm) with a repeating sequence that is complementary to that of the padlock probe. Subsequently, the DNA coils are post-labeled in a separate reaction step in high salt buffer at elevated temperature (typically for 20 min at 55°C) with magnetic nanobeads (size around 100 nm) conjugated with single-stranded DNA probes complementary to the repeating motif of the DNA coils. Binding of beads to DNA coils gives rise to a suppression of the AC magnetic susceptibility $\chi = \chi' - i\chi''$, where χ and χ are the in-phase and out-of-phase components of the AC susceptibility, respectively. More specifically, the binding of beads give rise to a decrease in amplitude of χ at the Brownian relaxation frequency of non-bound beads, χ''_{max}. Non-complementarity between the probes on the beads and the DNA coil sequence does not give rise to any measurable attractive binding interaction i.e. the AC magnetic susceptibility response is equal to that of a blank control sample (absence of DNA coils).[16] By utilizing a commercial AC susceptometer as read-out unit, we have demonstrated the versatility of this bioassay in several earlier studies.[17–19] We are currently focusing on developing a device, including automated sample preparation, for infectious diagnostics based on the bioassay principle using either a miniaturized AC susceptometer or a chip-based high-temperature superconducting quantum interference device. In connection to this work it is highly relevant to strive towards automation of the molecular protocol by investigating the possibilities for protocol simplifications.

Herein, the possibility of labeling DNA coils in real-time, i.e. adding magnetic nanobeads to the RCA mix with the intention to obtain bead-coil hybridization already during the RCA reaction, is evaluated. This approach, hereafter denoted as a combined protocol, aims at reducing the number of protocol steps as well as assay time and possibly also improving the limit of detection (LOD) of the assay. Also, a novel approach to analyze AC susceptibility data by recording the phase angle, $\xi = \arctan(\chi''/\chi')$, is investigated, avoiding the need of normalization of AC susceptibility data.

II. MATERIALS AND METHODS

Sequences of targets, padlock probes and detection oligonucleotides can be found in Table I. Note that concentrations of reagents given below, unless otherwise stated, refer to stock concentrations.

TABLE I. Oligonucleotide sequences. Segments of the detection probes hybridizing to the DNA coils are highlighted in red.

VC target	5' - CCC TGG GCT CAA CCT AGG AAT CGC ATT TG - 3'
VC padlock probe	5' - TAG GTT GAG CCC AGG GAC TTC TAG AGT GTA CCG ACC TCA GTA GCC GTG ACT ATC GAC TTG TTG ATG TCA TGT GTC GCA CCA AAT GCG ATT CC - 3'
Detection probe 1	5' - biotin - TTT TTT TTT TTT TTT TTT TTG TTG ATG TCA TGT GTC GCA CUU UU - 3'[a]
Detection probe 2	5' - biotin - TTT TTT TTT TTT TTT TTT TTG TTG ATG TCA TGT GTC GCA CCA AAT GCG ATT CC UU UU - 3'[a]

[a]The last four bases are 2'OMe-RNA.

A. Detection probe conjugation of magnetic nanobeads

40 μL of magnetic nanobead solution (BNF-Starch streptavidin, 100 nm, Micromod, Germany) of 10 mg/mL was washed two times with a special washing buffer (final composition of 10 mM Tris-HCl [Sigma-Aldrich, USA], 5 mM EDTA [Sigma-Aldrich], 0.1% Tween20 [Sigma-Aldrich], and 0.1 M NaCl [Sigma-Aldrich]). 2.49 μL of 10 μM detection probe solution (Biomers, Germany, 60 fold excess of probes with respect to the total number of beads) was added followed by incubation at room temperature during 15 min. Finally the bead suspension was washed two times with 1×phi29 buffer (Thermo Fisher Scientific, USA) and resuspended in 40 μL of 1×phi29 buffer (~10 mg/mL of beads). A shorter (probe 1, melting temperature T_m =54°C) and a longer (probe 2, T_m =75°C) detection probe hybridizing to the DNA coils by 22 and 35 bases, respectively, were examined in this study, see Table I.

B. Padlock probe ligation assay, rolling circle amplification and magnetic nanobead labeling of amplification products

A 50 μL ligation mix (20 nM of DNA circles in the final mix) was prepared by mixing 5 μL phi29-buffer (Thermo Fisher Scientific, 10×), 2.5 μL ATP (Thermo Fisher Scientific, 20 mM), 1 μL phosphorylated VC padlock probe (Biomers 1 μM), 3 μL VC target (Biomers, 1 μM), 1 μL T4 ligase (Thermo Fisher Scientific, 1 U/μL) and 37.5 μL MQ water, followed by 15 min incubation at 37°C. The resulting solution of ligated circles was diluted stepwise with 1×phi29 buffer to lower concentrations (8 nM and 2 nM).

For optimization of the combined protocol an RCA mix was prepared by mixing 0.5 μL ligated circles (or water in case of negative control), 5 μL phi29-buffer (10×), 3 μL dNTP (Thermo Fisher Scientific, 2.5 mM), 5 μL BSA (Thermo Fisher Scientific, 2 μg/μL), 1 μL phi29 polymerase (Thermo Fisher Scientific, 10 U/μL), 2 μL conjugated magnetic beads (10 mg/ml), 5 μL NaCl (0.5, 1 or 2 M) and 28.5 μL MQ water. The effect of NaCl in the amplification reaction was investigated by replacing NaCl with 33.5 μL MQ water as in the conventional RCA protocol. The RCA reaction was performed by incubation of the RCA mix at different temperatures (37, 45 or 50°C) and times (30, 45 or 60 min). This was followed by a final incubation end step at different temperatures (55 or 65°C) and times (0, 5, 10 or 20 min). Prior to magnetic read-out, 150 μL of Phosphate Buffered Saline (1×PBS, Sigma-Aldrich) was added.

To determine the LOD for the optimized combined protocol (detection probe 1, 100 mM final concentration of NaCl in the RCA mix) and for post-labeling (detection probe 1), an RCA master mix was prepared by mixing 150 μL phi29-buffer (10×), 90 μL dNTP (2.5 mM), 150 μL BSA (2 μg/μL), 150 μL NaCl (1M) and 855 μL MQ water. For the combined protocol 46.5 μL master mix, 0.5 μL ligated circles (20, 8, 2 nM) or water (in case of negative control), 1 μL phi29 polymerase (10 U/μL) and 2 μL of beads were mixed followed by incubation for 60 min at 37°C and an end step of 5 min at 55°C. 150 uL PBS was added prior to magnetic read-out. For post-labeling 46.5 μL master mix, 0.5 μL ligated circles (20, 8, 2 nM) or water (in case of negative control) and 1 μL phi29 polymerase (10 U/μL) were mixed followed by incubation for 60 min at 37°C and an end step of 5 min at 65°C. Thereafter 2 μL of beads were added followed by incubation for 20 min at 55°C and addition of 150 μL PBS prior to magnetic read-out.

As a post-labeling reference a batch of 4 nM DNA coils was prepared by mixing 10 μL of ligated circles (20 nM), 3 μL phi29 buffer (10×), 2 μL dNTP (2.5 mM), 3 μL BSA (2 μg/μL), 0.5 μL phi29 polymerase (10 U/μL) and 11.5 μL of MQ water followed by 60 min incubation at 37°C and an end step of 5 min at 65°C. 20 μL of a hybridization buffer solution (2 μL Tris-HCl pH 8.0 [1 M], 4 μL EDTA [0.5 M], 1 μL Tween-20 [10%], 10 μL NaCl [5 M] and 3 μL MQ water) was finally added and the 4 nM DNA coil solution was diluted stepwise with hybridization buffer to lower concentrations (8 nM and 2 nM). Post-labeling was done by adding 2 μL of beads to 50 μL of DNA coil solution followed by 20 min incubation at 55°C and addition of 150 μL PBS prior to magnetic read-out.

C. AC susceptometric read-out and data analysis

The frequency-dependent magnetic susceptibility, $\chi = \chi' - i\chi''$, was measured from 10 Hz to 100 kHz at room temperature in a commercial AC susceptometer system, DynoMag (Acreo,

Göteborg). Target quantification (dose-response curves) was accomplished in two ways; either by considering (i) the decrease of $\chi''_{\max}/\chi'_{high}$ upon increasing DNA coil concentration where χ'_{high} is the frequency independent high frequency limit of χ' (proportional to the iron-oxide content in the sample) or (ii) the decrease of the phase angle ξ at high frequencies upon increased DNA coil concentration.

III. RESULTS AND DISCUSSION

Figure 1 summarizes the results from the optimization of the combined protocol where the relative peak decrease of a 50 pM DNA coil sample compared to the negative control, i.e. $\left[\left[\chi''_{\max}/\chi'_{high}(NC) - \chi''_{\max}/\chi'_{high}(50pM)\right] / \left[\chi''_{\max}/\chi'_{high}(NC)\right]\right.$, is plotted versus different protocol parameters. A special notation is used to specify employed protocol parameters, $t_1@T_1+t_2@T_2$, where t_1 and t_2 denote the times (in minutes) for the RCA and the end step, respectively, and T_1 and T_2 are the corresponding temperatures (in °C). Panel (a) displays the relative peak decrease vs. NaCl concentration in the RCA mix where beads were conjugated with probe 1. Panel (b) shows the relative peak decrease vs. T_1 where the NaCl concentration in the RCA mix was 100 mM, t_1 =60 min, with or without a 5@55 end step and beads were conjugated with probe 2. Post-labeling reference points are also included. First of all, by comparing the relative peak decrease for post-labeling and 60@37+20@55 for 100 mM NaCl in panel (a), it can be concluded that the magnetic beads do not significantly interfere with the RCA reaction. Possible interference mechanisms could for instance be leakage of different kinds of metallic ions from the beads with an inhibitory effect on the phi29 enzyme or adsorption of enzyme on the bead surface. The lack of significant interference means that the starch casing of the beads is sufficient for the protocol. Furthermore, a comparison of the

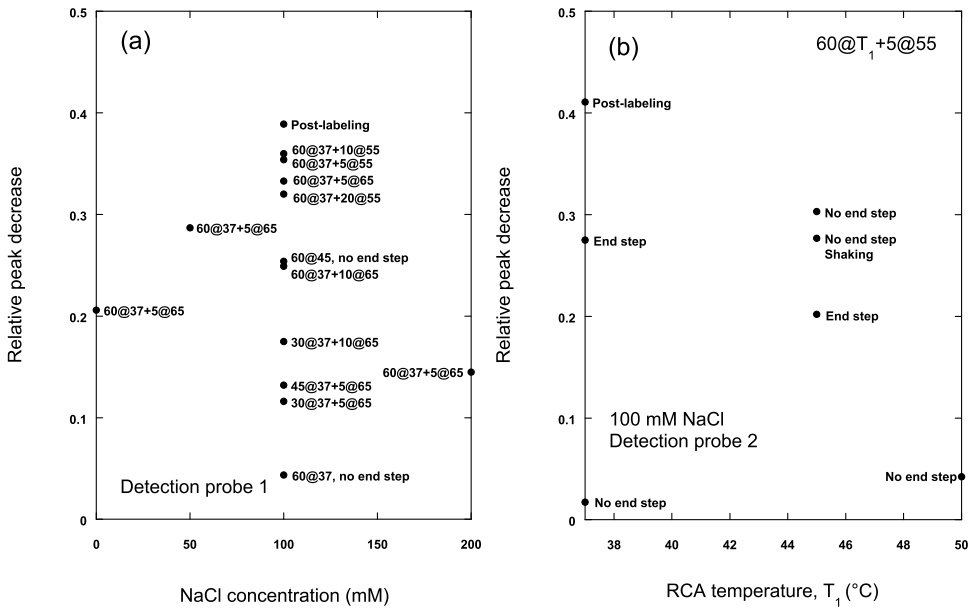

FIG. 1. Optimization of a biodetection protocol relying on the hybridization of detection probe-conjugated magnetic nanobeads (size 100 nm) to rolling circle amplification (RCA) products (DNA coils) with nanobeads present in the RCA reaction, i.e. a combined protocol. The combined protocol comprises the steps of running the RCA reaction for t_1 (min) at a temperature T_1 (°C), followed by a t_2 min end step during at an elevated temperature T_2 (°C). A notation "$t_1@T_1+t_2@T_2$" is used for these particular settings. Panel (a) displays the relative peak decrease (50 pM DNA coil sample compared to the negative control) vs. NaCl concentration in the RCA mix (beads conjugated with detection probe 1). Panel (b) shows the relative peak decrease vs. T_1 where the NaCl concentration in the RCA mix was 100 mM, t_1 =60 min, with or without a 5@55 end step (beads were conjugated with detection probe 2). Post-labeling refers to hybridizing the nanobeads to the DNA coils after completion of the RCA by employing 20 min of incubation at 55°C. Measurements were repeated once (qualitative interpretation).

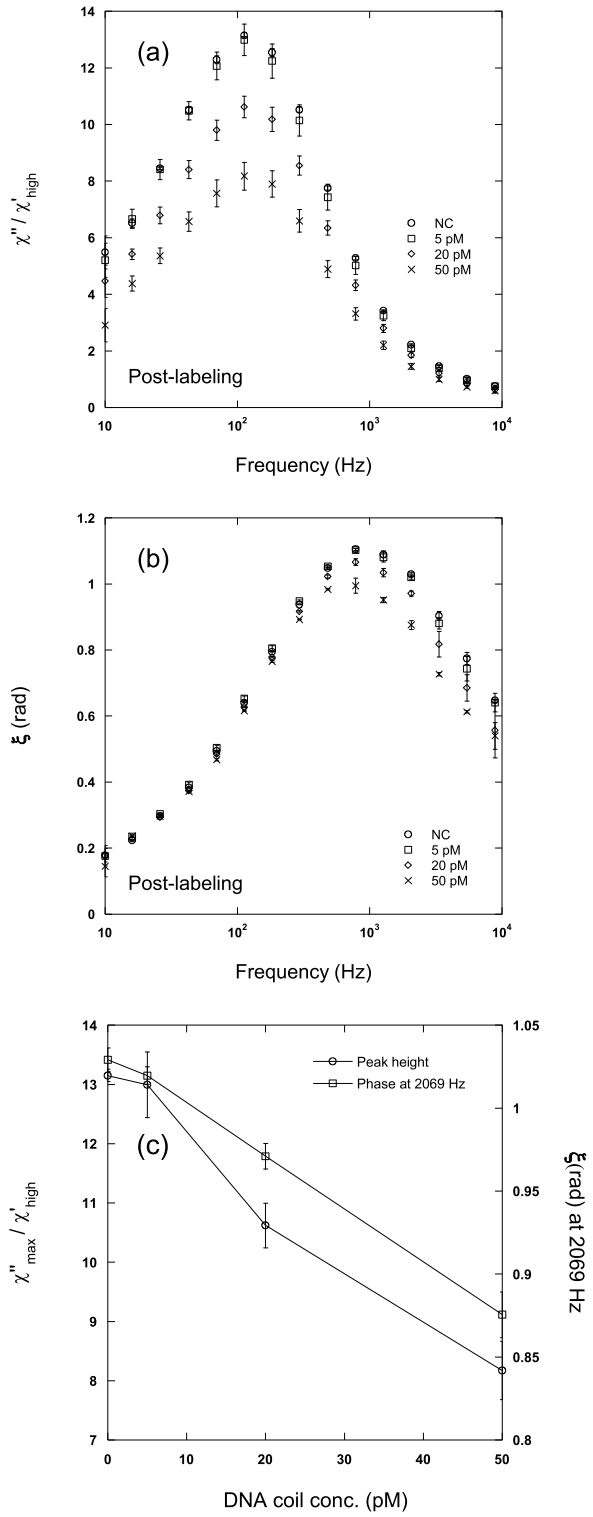

FIG. 2. Comparison of two methods used for obtaining dose-response curves from frequency-dependent magnetic susceptibility data ($\chi = \chi' - i\chi''$). The data correspond to post-labeling of DNA coils, using nanobeads with detection probe 1, a 60 min at 37°C RCA step followed by addition of beads and incubation for 20 min at 55°C prior to magnetic read-out. (a) χ'' spectra for different DNA coil concentrations normalized with respect to χ'_{high}, the frequency independent high frequency limit of χ'. (b) Phase angle, ξ, spectra for different DNA coil concentrations where $\xi = \arctan(\chi''/\chi')$. (c) Dose-response curves, viz. $\chi''_{\max}/\chi'_{high}$ (left y-axis) and ξ taken at 2069 Hz (right y-axis) vs. DNA coil concentration. Error bars represent one standard deviation based on three independent measurements.

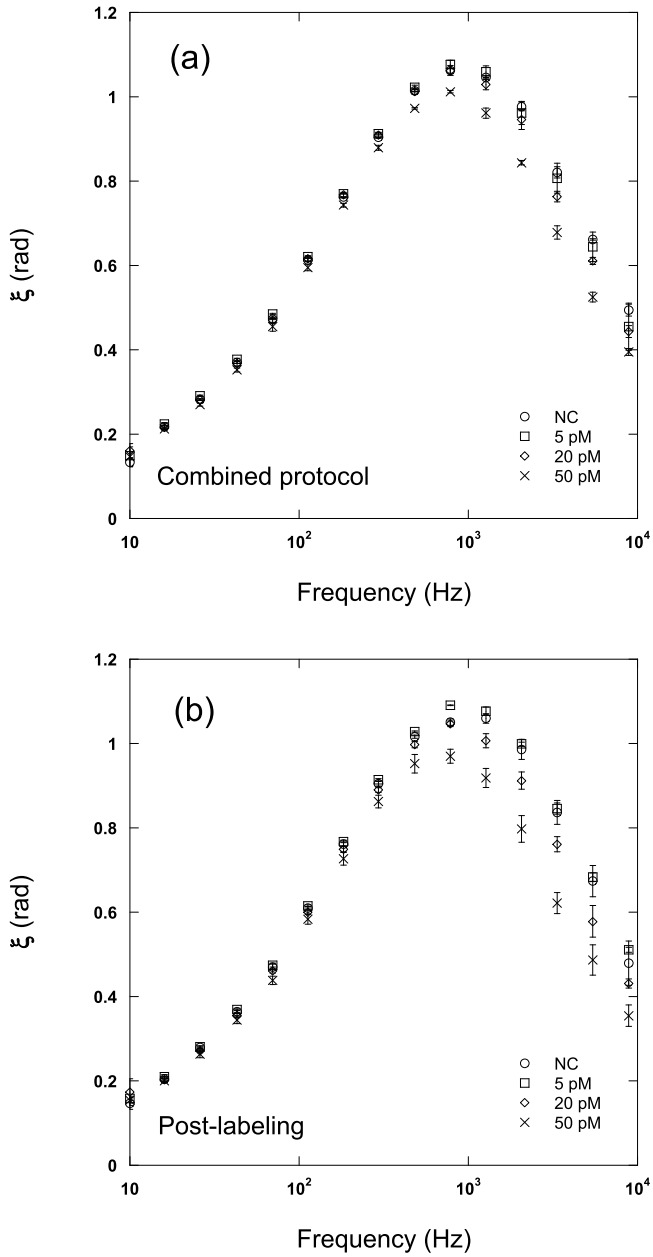

FIG. 3. Phase angle vs. frequency for different DNA coil concentrations for (a) the optimized combined protocol (RCA for 60 min at 37° C with beads present and with 100 mM of NaCl followed by a 5 min at 55°C end step) and (b) for post-labeling (RCA for 60 min at 37°C in absence of beads and with 100 mM of NaCl followed by addition of beads and a 20 min at 55°C end step). Nanobeads were conjugated with detection probe 1. Error bars represent one standard deviation based on three independent measurements.

60@37+5@65 points in panel (a) indicates that a NaCl concentration of about 100 mM is optimal for the RCA reaction. The existence of an optimum is the result of a compromise between two competing factors; viz. 1) the decrease in number and average length of DNA coils due to suppression of the enzymatic activity of the polymerase in the presence of NaCl and 2) the increase in bead-coil hybridization efficiency upon increasing NaCl concentration. It can also be concluded from panel (a) (by comparing the different 100 mM NaCl samples) that an insignificant number of beads hybridize to the DNA coils while the RCA reaction is ongoing and, consequently, that the major part of the bead-coil binding occurs during the end step.

It is further found that an end step temperature of 55°C, which is close to the melting temperature of detection probe 1, is more appropriate to use than the higher temperature of 65°C; as the relative peak decrease for 60@37+10@55 and 60@37+5@55 is larger than for 60@37+10@65 and 60@37+5@65. There is also a trend of a decreasing amount of hybridized beads upon decreasing RCA time. For T_2 = 55°C it can be concluded that t_1 = 5 min is enough to reach a steady state in the bead-coil binding reaction (the relative peak decrease for 60@37+5@55 and 60@37+10@55 are almost equal) and the amount of bound beads is nearly identical to that of post-labeling. In order to further explore the possibility to achieve bead-coil binding during the RCA process, a longer detection probe was evaluated, see panel (b). It was hypothesized that a detection probe with a higher T_m would be able to hybridize more efficiently to the RCA product at 37°C during amplification. Clearly, however, this is not the case and including an end step is also found to be necessary in this case. The most likely explanation for this phenomenon is that the rate of the amplification reaction and the coiling up of the single stranded RCA product is higher than that of the hybridization reaction between the detection probes and the RCA products, thereby not substantially increasing the number of available probe binding sites. Alternatively, there is a possibility that bead-coil hybridization occurs at a very early stage of the RCA process and that these bound beads sterically inhibit binding of additional beads while the DNA coils continue growing. DNA coils growing around bound beads could cause such steric hindrance since the beads hybridize to the DNA coils in a multivalent manner. A slight increase of T_1 from 37 to 45°C does not improve the performance of the assay when an end step is used, while a significant improvement is obtained in the no-end-step case. Introducing gentle shaking of the RCA mix during the RCA reaction in the no-end-step experiments did not improve the bead-coil binding efficiency. Furthermore, T_1 = 50°C is obviously too high temperature for the phi29 enzyme. Conclusively, it was found that a combined protocol with 60@37+5@55 conditions is optimal to use with nanobeads equipped with probe 1.

Figure 2 presents a comparison between the two methods used for obtaining dose-response curves from frequency-dependent magnetic susceptibility spectra measured on samples prepared by post-labeling (as described in the last paragraph of section II, part B). Panels (a) and (b) show normalized χ'' spectra and phase angle spectra, respectively, for different DNA coil concentrations. Panel (c) displays dose-response curves, viz. $\chi''_{\max}/\chi'_{high}$ (left y-axis) and phase angle taken at 2069 Hz (right y-axis) vs. DNA coil concentration. Apparently, the two methods give the same LOD (20 pM) but phase angle analysis constitutes a more convenient approach since the normalization of $\chi''_{\max}$ with respect to χ'_{high} can be avoided. Target quantification based on the phase angle method could also be performed by measuring the susceptibility at one single frequency. Thereby the read-out time in the DynoMag system would be substantially reduced and limited to about 2 min.

Based on the observation that the major part of the bead-coil hybridization in the combined protocol occurs during the end step, the LOD is expected to be comparable with post-labeling. This statement is confirmed by the results presented in Fig. 3 showing phase angle versus frequency spectra for the optimized combined protocol (a) and for post-labeling (b). It can be seen that the LOD equals 20 pM for both protocols. Compared to the previously used post-labeling protocol the combined protocol is faster and easier to automate.

IV. CONCLUSION

In this paper, possibilities for protocol simplifications for a biodetection principle relying on hybridization of probe-functionalized magnetic nanobeads to rolling circle amplification products have been evaluated. It can be concluded that beads can be present during amplification without noticeably interfering with the phi29 enzyme and that bead-coil hybridization subsequently is achieved during an end step at elevated temperature within just a few minutes prior to read-out in an AC susceptometer setup. Therefore one reaction step requiring an additional reagent handling step can be avoided, facilitating assay integration into automated formats. The reason for why the major part of bead-coil hybridization occurs during the end step and not during the RCA reaction is most likely related to that the rate of the RCA reaction and coiling up of the single stranded RCA product is higher than that of the hybridization reaction between the detection probes and the RCA products. Moreover, by recording the phase angle at a single frequency the total assay time for the optimized

combined protocol (including padlock probe ligation, amplification, labeling and read-out) would be no more than 1.5 hours which is clinically relevant for a number of diagnostic applications,

ACKNOWLEDGMENTS

This work was financially supported by Swedish Research Council Formas (project number 221-2012-444 and 2011-1692) and the Swedish Foundation for Strategic Research (project number SBE13-0125).

[1] M. Holzinger, A. Le Goff, and S. Cosnier, Front. Chem. **2**, 63 (2014).
[2] D. Issadore, Y.I. Park, H. Shao, C. Min *et al.*, Lab on a Chip **14**, 2385 (2014).
[3] J. Llandro, J.J. Palfreyman, A. Ionescu, and C.H.W. Barnes, Med. Biol. Eng. Comput. **48**, 977 (2010).
[4] T.A.P. Rocha-Santos, Trac-Trend Anal. Chem. **62**, 28 (2014).
[5] A.P.F. Turner, Chem. Soc. Rev. **42**, 3184 (2013).
[6] J.O. Tegenfeldt, C. Prinz, H. Cao, R.L. Huang *et al.*, Anal. Bioanal. Chem. **378**, 1678 (2004).
[7] B. Srinivasan and S. Tung, J. Lab. Autom. **20**, 365 (2015).
[8] A. van Reenen, A.M. de Jong, J.M.J. den Toonder, and M.W.J. Prins, Lab on a Chip **14**, 1966 (2014).
[9] A. Rios, M. Zougagh, and M. Bouri, Anal. Methods-Uk **5**, 4558 (2013).
[10] D. Ivnitski, I. Abdel-Hamid, P. Atanasov, and E. Wilkins, Biosens. Bioelectron. **14**, 599 (1999).
[11] P. Arora, A. Sindhu, N. Dilbaghi, and A. Chaudhury, Biosens. Bioelectron. **28**, 1 (2011).
[12] P. Leonard, S. Hearty, J. Brennan, L. Dunne *et al.*, Enzyme Microb. Tech. **32**, 3 (2003).
[13] S.X. Wang and G. Li, IEEE Trans. Magn. **44**, 1687 (2008).
[14] J. Connolly and T.G. St Pierre, J. Magn. Magn. Mater. **225**, 156 (2001).
[15] A.P. Astalan, F. Ahrentorp, C. Johansson, K. Larsson *et al.*, Biosens. Bioelectron. **19**, 945 (2004).
[16] M. Strömberg, J. Göransson, K. Gunnarsson, M. Nilsson *et al.*, Nano Letters **8**, 816 (2008).
[17] M. Strömberg, T. Zardán Gómez de la Torre, M. Nilsson, P. Svedlindh *et al.*, Biotechnol. J. **9**, 137 (2014).
[18] T. Zardán Gómez de la Torre, A. Mezger, D. Herthnek, C. Johansson *et al.*, Biosens. Bioelectron. **29**, 195 (2011).
[19] A. Engström, T. Zardán Gómez de la Torre, M. Strømme, M. Nilsson *et al.*, Plos One **8**, e62015 (2013).